Journal of Physics: Conference Series **209** (2010) 012018 doi:10.1088/1742-6596/209/1/012018

Simulation supported analysis of the effect of SiN_x interlayers in AlGaN on the dislocation density reduction

O Klein[1], J Biskupek[1], U Kaiser[1], K Forghani[2], S B Thapa[2] and F Scholz[2]

[1] Central Facility of Electron Microscopy, Ulm University, 89081 Ulm, Germany
[2] Institute of Optoelectronics, Ulm University, 89081 Ulm, Germany

E-mail: oliver.klein@uni-ulm.de

Abstract. SiN_x interlayers can act as anti-surfactants and drastically reduce the dislocation density in pure GaN layers. In our work we could observe a very efficient dislocation annihilation of the **a**-type threading dislocations (TD) at a fractional SiN_x monolayer even in $Al_xGa_{1-x}N$ layers with relatively high Al content of x=0.2, grown on c-plane sapphire by MOVPE. The investigations were focused on the effect of the SiN_x interlayer on the dislocation density reduction of the **a**-type TDs. Weak-beam dark-field (WBDF) and high-resolution (HR) TEM analyses directly at the SiN_x interface indicate that the most frequently occurring effect for the reduction of the **a**-type TDs is the conversion of an **a**-type TD into an **a**-type basal dislocation due to lateral overgrowth of SiN_x by AlGaN. To confirm this effect, an appropriate dislocation model was developed for the **a**-type TD in AlGaN and its bending due to the SiN_x nano-mask. Corresponding image calculations were performed and compared with the experiments.

1. Introduction

In recent years aluminium nitride (AlN) has attracted much attention due to its extremely large direct band gap of approximately 6.0 eV and its impressive chemical and thermal stability. Thus AlN and $Al_xGa_{1-x}N$ ternary alloys are promising materials for high-power high temperature electronic applications and optoelectronic devices in the UV range. As group-III nitride wafers are still not available in sufficient amount and quality, AlN has to be grown on foreign substrates such as Al_2O_3 (sapphire). Unfortunately the large lattice mismatch between the AlGaN/Al_2O_3 interface of up to -14% leads to the formation of strain induced misfit dislocations at the interface, which are the cause of the generation of threading dislocations (TD), inducing a high dislocation density in the range of $10^{10}cm^{-2}$ and decreasing the crystal quality [1, 2]. As published among others in [3, 4], a promising possibility to reduce the dislocation density at the surface of an AlGaN layer system is the growth of intermediate SiN_x layers. SiN_x can act as an anti-surfactant and drastically reduce the dislocation density in AlGaN layers with high gallium content by lateral overgrowth. In our work we could observe a very efficient dislocation annihilation of the **a**-type TDs at a fractional SiN_x monolayer even in $Al_xGa_{1-x}N$ layers with a relatively high Al content of x=0.2. However, the annihilation effect of the pure edge **a**-type TDs does not occur homogenously over the whole SiN_x interface in our sample. Regions of the SiN_x layer at which the propagation of the **a**-type TDs is completely stopped alternate with regions where almost no annihilation effect was observed, which motivated further studies on the SiN_x monolayer and its effect on the dislocation reduction. Analyses regarding the annihilation process were carried out by exploiting the weak-beam dark-field (WBDF) method and by high-resolution TEM investigations of the a-type TDs directly at the SiN_x interface. The investigations were supported by an

appropriate dislocation model, developed for comparative image calculations by the multislice algorithm.

2. Experimental methods

2.1. Investigated samples and layer growth

Our investigations centered on two different samples, denoted by S1 and S2 in this work. Sample S1 is composed of a 1.2 µm thick $Al_{0.2}Ga_{0.8}N$ layer with an in-situ deposited intermediate nominal SiN_x monolayer [5] using silane (SiH_4) as precursor with a deposition time of 4 minutes, located 150 nm above the substrate. It was grown by low pressure MOVPE at a temperature of 1120°C and a pressure of 80 hPa. Sample S2 consists of a pure 500 nm thick AlN layer grown at 1190°C and 35 hPa [2, 6, 7]. It was used for comparative WBDF and HRTEM pre-investigations, to prove the developed dislocation model for the pure edge **a**-type TD in wurtzite group-III nitrides. For both samples the actual layer growth was preceded by the deposition of a low temperature 20 nm thick oxygen doped AlN:O nucleation layer, to improve the crystal quality [8]. Trimethylaluminium/-gallium (TMAl/Ga) and NH_3 were used as group III and V precursors, respectively.

2.2. TEM measurements

Thin TEM foils were prepared for investigation in cross-sectional and plan-view geometries using standard techniques including mechanical polishing and low-angle argon thinning [9]. To image the dislocations and distinguish the different dislocation types, cross-sectional WBDF images close to the [01-10] zone were analysed by exploiting the **g·b** criterion. The WBDF method was carried out under the 3**g** condition. In wurtzite 2H group-III nitrides perfect dislocations can exist with three different types of Burgers vectors **b**: **a**-type TDs with **b** of type 1/3 [2-1-10], **c**-type TDs with **b** = [0001] and (**a+c**)-type TDs with **b** of type 1/3 [2-1-13]. Since most of the growth induced TDs in epitaxially deposited AlGaN layers propagate parallel to the [0001] direction, **a**-type TDs are pure edge dislocations, whereas **c**-type TDs are pure screw dislocations. The Burgers vector of a mixed TD propagating parallel to the c-axis is of type (**a+c**). According to the **g·b** criterion, only **c**-type and (**a+c**)-type dislocations are visible in the WBDF image when using the 0002 reflection. Exploiting the 2-1-10 reflection, only **a**-type and (**a+c**)-type TDs give rise to a contrast. To determine Burgers vectors directly, HRTEM images were recorded at the [01-10] zone as well as in the [0001] plan-view projection. The investigations were carried out with a Philips CM-20 microscope.

2.3. Model generation and image calculation

The atomic dislocation models for comparative image calculations were developed with the aid of the Hypercube Hyperchem™ software package [10]. The dislocations were placed manually into the bulk crystal system according to our experimental investigations by performing an appropriate Volterra construction [11]. The subsequent relaxation of the supercell was realised after a geometry optimization of up to 27000 atoms by using a conjugate gradient molecular mechanic algorithm with an MM+ type force field. The image calculations were carried out by performing multislice calculations using the Musli software under CM-20 conditions with a Cs value of 1.2 mm and a high-tension of 200 kV [12].

3. Results and discussion

3.1. Pre-investigations and general properties of SiN_x interlayers in AlGaN

The bright field (BF) image in Figure 1a shows an overview of the dislocation structure in sample S1, in which the TDs of all types are visible. There are regions at the SiN_x layer where the propagation of the TDs is completely stopped and the annihilation process is highly efficient (lower arrows). However this does not apply to all regions of the specimen. The WBDF images (b) and (c) are recorded from the same sample area by exploiting the 2-1-10 and the 0002 reflection, respectively.

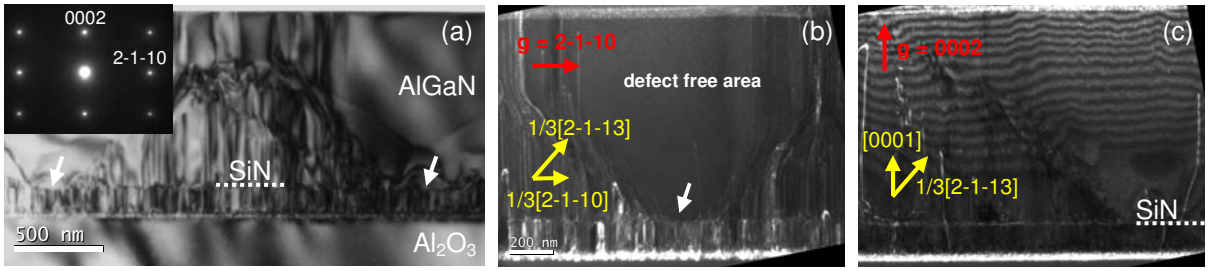

Figure 1. TEM cross-sectional views of sample S1. The BF image (a) from the [01-10] zone axis shows regions of the SiN_x layer at which the dislocation annihilation is highly efficient (bottom arrows in (a) and (b)), whereas the propagation of the TDs is not stopped in other regions. The WBDF images are recorded from the same sample area, exploiting the 2-1-10 (b) and the 0002 reflection (c). The Burgers vectors of the TDs visible in the respective WBDF image are also charted. In general, the sample shows a very high density of pure edge **a**-type TDs beneath the SiN_x layer (b), whereas the number of screw and mixed TDs is very small (c). Thus the appearance of large defect free areas is primarily based on the bending and annihilation of the pure edge **a**-type TDs at the SiN_x layer.

They illustrate a very high density of pure edge **a**-type TDs below the SiN_x interlayer, whereas the number of **c**- and (**a**+**c**)-type dislocations is very small. Thus the most frequently occurring effect of the SiN_x layer is the annihilation of the pure edge **a**-type TDs. A remarkable feature is the bending of the **a**-type TDs at regions close to the annihilation zone above the SiN_x interface, whereas the general bending direction always points away from the region with high annihilation efficiency. Furthermore the dislocation bending decreases with increasing distance from the zone of high annihilation grade. This bending effect and the annihilation of the **a**-type TDs at the SiN_x interface lead to the formation of large defect free areas.

In this work our investigations centered on the annihilation process at the SiN_x interlayer itself. As dislocation lines can not start or stop inside the crystal [11], they are always closed loops or end at surfaces. Thus, the TDs have to change the direction to become basal dislocations, propagating parallel to the surface and getting annihilated by interaction, to reduce the dislocation density at the surface of an epitaxially grown heterostructure. This effect is provided by the SiN_x interlayer. As we know from [4, 13], the growth of SiN_x on AlGaN is promoted at the dislocation cores due to free bonds. The treatment of the AlGaN layers with SiH_4 and NH_3 leads to a fractional coverage of the surface of the layers with SiN_x and causes the formation of a SiN_x nano-mask with SiN_x islands and exposed AlGaN regions (figure 2a). As SiN_x acts as an anti-surfactant, the SiN_x islands are laterally overgrown by the subsequent AlGaN layers. Thus, the two-dimensional epitaxial growth of AlGaN switches to a three-dimensional insular growth with lateral overgrowth of the SiN_x. The changing of the vertical growth direction to a lateral growth direction leads to the conversion of the a-type TDs into basal dislocations. The WBDF images of S1 in Figure 2b & c close to the SiN_x region show this effect for **a**-type and **c**-type TDs, respectively. The dislocation bending indicates the changing of the ratio between lateral and vertical growth at the SiN_x interface. If the dislocation density is sufficiently high, the dislocation bending leads to the annihilation of the TDs by the formation of dislocation

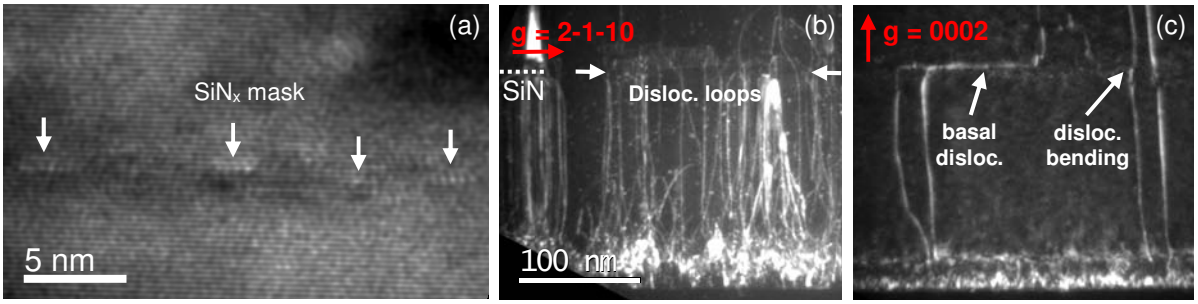

Figure 2. HRTEM (a) and WBDF micrographs of sample S1 in the area of the SiN_x interface at a zone of high annihilation grade. Image (a) illustrates the fractional coverage of AlGaN with SiN_x (Si deposition indicated by arrows). The bending of the **a**-type TDs and the annihilation by the formation of dislocation loops is clearly visible in image (b). Image (c) shows the propagation of the TDs with screw component. Even there, the conversion of the TDs into basal dislocations leads to an interaction of the TDs.

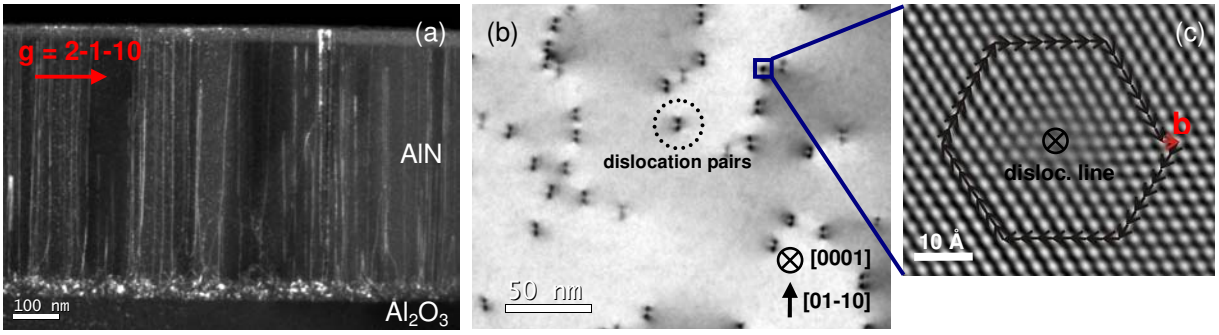

Figure 3. Cross-sectional WBDF image of S2 shows pure edge **a**-type TDs in AlN (a). In the [0001] plan-view image the arrangement of the **a**-type TDs in pairs along the [01-10] direction is clearly visible (b). This dislocation structure exactly corresponds to the Volterra cut along the [01-10] direction. The unclosed Burgers circulation around the dislocation core in the Fourier filtered HRTEM micrograph definitely identifies the TD as a pure edge **a**-type TD with Burgers vector **b** = 1/3 [2-1-10] (c).

loops. Otherwise the TD cannot interact after the bending and will continue to propagate parallel to the c-axis due to the increasing epitaxial growth with increasing distance to the SiN_x interface.

According to the annihilation process of the pure edge **a**-type TDs in 2H AlGaN, there is one possible mechanism for the conversion of such dislocations into basal dislocations at the SiN_x interface by lateral overgrowth. This is the bending of a pure edge **a**-type TD with $\mathbf{b}_1$ = -1/3 [2-1-10] to a pure edge **a**-type basal dislocation at the SiN_x interface, propagating parallel to the surface. This dislocation with Burgers vector $\mathbf{b}_3 = \mathbf{b}_1$ can interact with an adjacent pure edge **a**-type TD with $\mathbf{b}_2$ = 1/3 [2-1-10] and is therefore annihilated by the formation of a closed dislocation loop. Referring to the Volterra construction, this corresponds to the insertion of an additional (2-1-10) plane into the crystalline system. The developed dislocation model in our work is based on this relation and was verified by comparing experimental TEM studies with calculated images, exploiting the multislice algorithm.

3.2. Development and verification of the dislocation model for the pure edge a-type TD in Al(Ga)N

The dislocation model for the pure edge **a**-type TD in 2H Al(Ga)N was developed with the help of WBDF and HRTEM investigations on sample S2, by comparing the experimental images with the calculated ones, obtained by applying the multislice algorithm on the dislocation model. Beside the cross-sectional WBDF investigations (figure 3a), the plane-view BF and HRTEM micrographs indicate, that the formation of the pure edge **a**-type TDs in Al(Ga)N can be described as a cut along the [01-10] direction with a subsequent displacement at **b** = 1/3 [2-1-10] according to the Volterra construction. This construction rule is verified by the formation of dislocation pairs orientated along

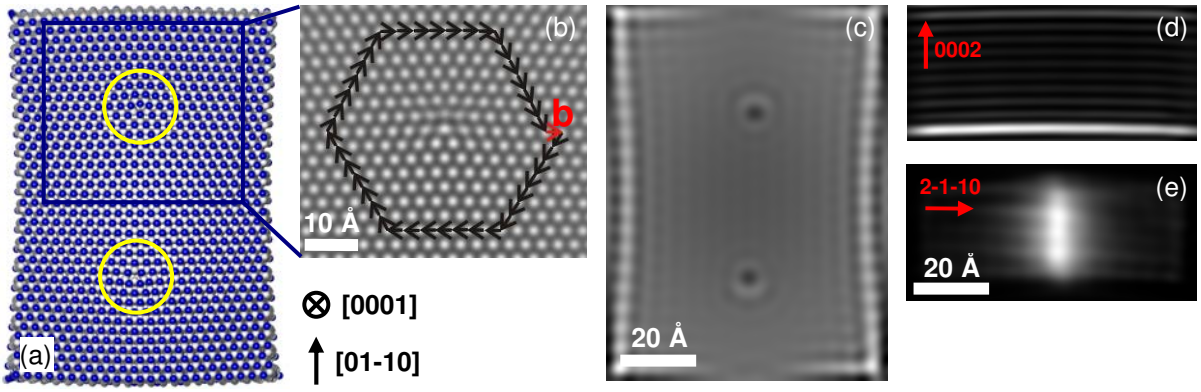

Figure 4. Atomic model for the edge **a**-type TD pair in Al(Ga)N (a) and calculated images (b-e) by applying the multislice algorithm on the model. In accordance with our TEM measurements, the HRTEM calculation identifies the dislocation as a pure edge **a**-type TD with **b** = 1/3 [2-1-10] (b). In the [0001] BF calculation the dislocation pair is clearly visible, as it was observed in our plane-view TEM investigations (c). Also the WBDF calculations and the verification of the **g**·**b** criterion are consistent with the experiment (d, e).

the [01-10] direction, clearly visible in the plan-view BF and HRTEM investigations (figure 3b & c).

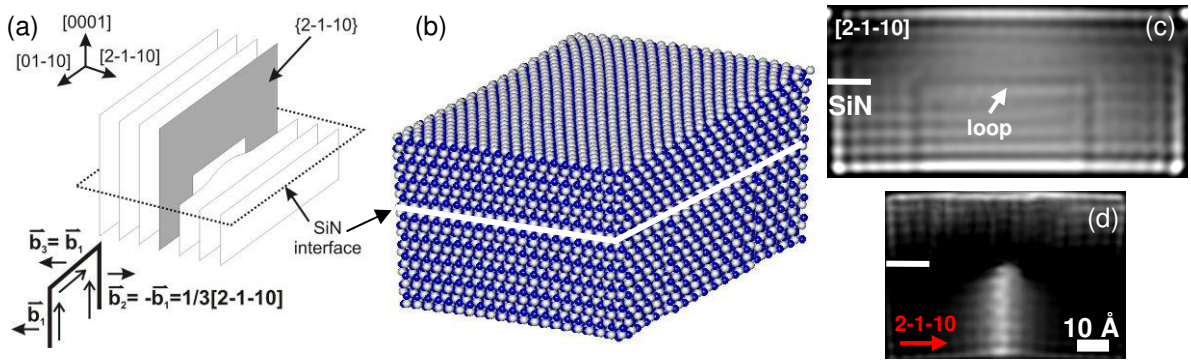

Figure 5. Extended atomic model for the annihilation process of **a**-type TDs in Al(Ga)N at the SiN_x interface by the formation of a dislocation loop (a, b). The BF calculation at the [2-1-10] zone clearly shows the dislocation loop created by an **a**-type basal dislocation (c). In the WBDF calculation close to the [01-10] zone the propagation of the dislocation line seems to end at the SiN_x interface as it was observed in figure 2b (d).

According to these results, it was now possible to construct the dislocation model for the pure edge **a**-type TD in Al(Ga)N. Figure 4 shows the relaxed model of the supercell after geometry optimization of around 17000 atoms and the image calculations applied to the model as described in chapter 2.3. We received the filled–core model for the pure edge **a**-type TD, representing a known core-type in 2H Al(Ga)N [14]. The WBDF calculations under the 3**g** condition close to the [01-10] zone verify the **g**·**b** criterion (figure 4d, e). The dislocation line is clearly visible by exploiting the 2-1-10 reflection, whereas the TD produces no contrast when using **g** = 0002. The consistence of the calculated images with our experimental investigations confirms the applicability of the construction rule for the formation of pure edge **a**-type TDs in Al(Ga)N and gives reason to extend the dislocation model in terms of the annihilation process at the SiN_x layer as we mentioned already in the previous chapter.

Figure 5a & b shows the atomic model for the annihilation process of the **a**-type TDs in Al(Ga)N at the SiN_x interface by the formation of a pure edge **a**-type basal dislocation due to lateral overgrowth, whereas SiN_x was not explicitly implemented in the model. The interaction of the basal dislocation with an **a**-type TD leads to the formation of a loop. Thus, the dislocation pair stops to propagate towards the surface. The relaxed model of the supercell contains around 27000 atoms. The calculated BF image at the [2-1-10] zone in figure 5c clearly shows the formation of the loop. Besides, the

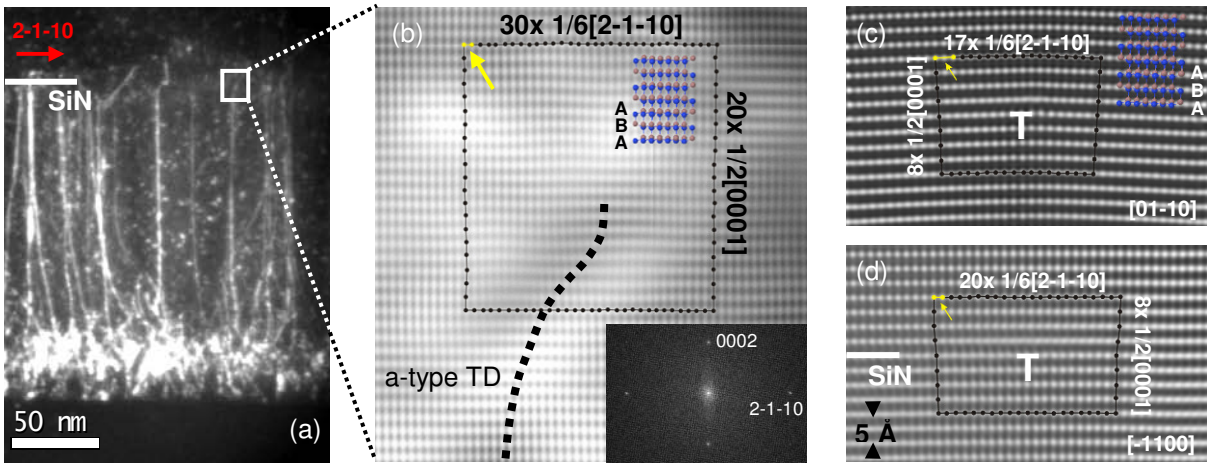

Figure 6. Burgers vector analysis of an annihilated pure edge **a**-type TD (a) at the SiN_x interlayer and comparison with HRTEM multislice calculations. The unclosed Burgers circulation in the filtered HRTEM image (b) results in a Burgers vector of 1/6[2-1-10] in the imaged projection. Thus, the dislocation line of the TD gets a component perpendicular to the image plane at the SiN_x interface. The unclosed circulation in the calculated image at the [01-10] zone (c) shows the Burgers vector 1/3[2-1-10] of the **a**-type basal dislocation, as provided in the model. In accordance to (b) we receive a Burgers vector of 1/6[2-1-10] in the calculated image from the [-1100] zone, corresponding to the imaging of the **a**-type Burgers vector from a 60° projection.

propagation of the TD is stopped as it was observed in our cross-sectional TEM investigations, clearly visible in the WBDF calculation by exploiting the 2-1-10 reflection (figure 5d).

The verification of the dislocation model was further carried out by comparing calculated and experimental HRTEM images at the SiN_x interface, where the dislocation bending and annihilation takes place due to lateral overgrowth. The experimental HRTEM investigations at the SiN_x nano-mask in the area of an annihilated pure edge **a**-type TD and the HRTEM image calculations on the developed model are in very good agreement according to the Burgers vector analysis. The simulation supported investigations in figure 6 show, that the annihilation of the pure edge **a**-type TDs in Al(Ga)N is realised by the conversion of an **a**-type TD into an **a**-type basal dislocation and subsequent interaction with an adjacent **a**-type TD due to lateral overgrowth of the SiN_x anti-surfactant.

4. Summary and conclusions

A detailed TEM study on the annihilation process of the **a**-type TDs at the SiN_x nano-mask in MOVPE grown Al(Ga)N layers on sapphire has been presented. We could partly observe a very efficient dislocation annihilation of the **a**-type TDs at the SiN_x interface even in $Al_xGa_{1-x}N$ layers with a relatively high Al content of x=0.2. Our supposed dislocation model explained the propagation of the **a**-type TD in the Al(Ga)N layer and at the SiN_x interface. It is shown by our simulation supported HRTEM and WBDF analyses, that the most frequently occurring effect for the reduction of the **a**-type TDs is the conversion of an **a**-type TD into an **a**-type basal dislocation at the SiN_x interface due to lateral overgrowth of the SiN_x by AlGaN. After bending, the basal dislocation can be annihilated by interacting with another **a**-type dislocation. The consistence of the calculated images with our experimental investigations confirms the applicability of the developed atomic dislocation model to the propagation of the **a**-type TDs at the SiN_x interface in the investigated crystal system.

Acknowledgements

We like to thank S. Grözinger for the sample preparation and J. Hertkorn, S. Schwaiger, F. Lipski for assistance in MOVPE growth. This work was partly financially supported by the Bundesministerium für Bildung und Forschung (BMBF) and the Deutsche Forschungsgemeinschaft (DFG).

References

[1] Kuwano N, Tsuruda T, Kida Y, Miyake H, Hiramatsu K and Shibata T 2003 *Physica Status Solidi (c)* **7**, 2444-7
[2] Thapa S B, Kirchner C, Scholz F, Prinz G M, Thonke K, Sauer R, Chuvilin A, Biskupek J, Kaiser U and Hofstetter D 2007 *Journal of Crystal Growth* **298**, 383
[3] Engl K*, et al.* 2006 *Journal of Crystal Growth* **289**, 6
[4] Tanaka S, Takeuchi M and Aoyagi Y 2000 *Jpn. J. Appl. Phys.* **39**, 831
[5] Hertkorn J, Lipski F, Brückner P, Wunderer T, Thapa S B, Scholz F, Chuvilin A, Kaiser U, Beer M and Zweck J 2008 *Journal of Crystal Growth* **310**, 4867
[6] Thapa S B, Hertkorn J, Scholz F, Prinz GM, Feneberg M, Schirra M, Thonke K, Sauer R, Biskupek J and Kaiser U 2008 *Physica Status Solidi (a)* **5**, 1774
[7] Thapa S B*, et al.* 2008 *Journal of Crystal Growth* **310**, 4939-41
[8] Hertkorn J, Bruckner P, Thapa S B, Wunderer T, Scholz F, Feneberg M, Thonke K, Sauer R, Beer M and Zweck J 2007 *Journal of Crystal Growth* **308**, 30
[9] Radnoczi G and Barna A 1996 *Surf. Coat. Technol.* **80**, 89
[10] Hypercube 2002 HyperChem™ Release 7 for Windows.
[11] Hirth JP and Lothe J 1982 *Theory of Dislocations* (New York: Wiley)
[12] Chuvilin A and Kaiser U 2005 *Ultramicroscopy* **104**, 73
[13] Elsner J, Jones R, Sitch P K, Porezag VD, Elstner M, Frauenheim T, Heggie MI, Öberg S and Briddon PR 1997 *Physical Review Letters* **79**, 3672
[14] Blumenau AT, Fall CJ, Elsner J, Jones R, Heggie M I and Frauenheim T 2003 *Physica Status Solidi (c)* **6**, 1684